Available online at www.sciencedirect.com
SCIENCE DIRECT®
Pergamon
Materials Research Bulletin 38 (2003) 1979–1986
Materials Research Bulletin
www.elsevier.com/locate/matresbu

Physical and chemical properties of nanosized powders of gadolinia-doped ceria prepared by the cation complexation technique

R.A. Rocha*, E.N.S. Muccillo

Centro Multidisciplinar para o Desenvolvimento de Materiais Cerâmicos CCTM, Instituto de Pesquisas Energéticas e Nucleares, C.P. 11049, Pinheiros, São Paulo 05422-970, SP, Brazil

Received 25 April 2003; received in revised form 18 August 2003; accepted 5 September 2003

Abstract

Ceria-gadolinia solid solutions were prepared by the cation complexation technique using citric acid as complexant agent. The main purpose of this work was to evaluate the calcining profile of the precursor material in order to obtain nanosized powders with high sinterability. The main results show that powders with less than 10 nm of crystallite size may be obtained at relatively low temperatures. Pressed specimens attained a relative density >99% after sintering at 1500 °C for 3 h.
© 2003 Elsevier Ltd. All rights reserved.

Keywords: A. Ceramics; B. Sol–gel; C. Infrared spectroscopy; C. X-ray diffraction

1. Introduction

Ceria and rare earth doped ceria powders have a number of important applications in catalysts, abrasives, solid oxide fuel cell (SOFC) systems, and gas sensors [1,2]. Alkaline earth and rare earth oxides have high solubility in cerium oxide forming substitutional solid solutions. The introduction of aliovalent cations gives rise to oxygen vacancies as charge compensating defects thereby enhancing the ionic conductivity. At 1400 °C, the gadolinium oxide is 100% soluble in ceria [3], and its ionic conductivity is one of the highest among these solid electrolytes [4]. Gadolinia-doped ceria is one of the ceria-based solid solutions proposed for intermediate temperature application of SOFC [5].

These solid solutions can be synthesized by a variety of techniques such as conventional powder mixing [6,7], co-precipitation [8–11], and hydrothermal recrystallization [12]. In general, chemical techniques have the advantage over conventional techniques that the precursor presents high reactivity

* Corresponding author. Tel.: +55-11-38169357; fax: +55-11-38169370.
E-mail address: rarocha@ipen.br (R.A. Rocha).

0025-5408/$ – see front matter © 2003 Elsevier Ltd. All rights reserved.
doi:10.1016/j.materresbull.2003.09.025

allowing a reduction in the sintering temperature and/or time. Earlier works [9,13–15] using polymeric precursors techniques for the preparation of ceria solid electrolytes have shown that it was necessary to employ high temperatures (>1500 °C) and times (>5 h), or to introduce a milling step after calcination, to attain a high densification. In these previous works, the polymeric precursor was prepared by the Pechini [16] method using tartaric acid and ethylene glycol [9], or citric acid and ethylene glycol [13] for the polymerization. Alternatively, an organic precursor can be prepared by using ethylene glycol as complexant agent without the polyesterification reaction [14,15].

In this work, a variant of the sol–gel technique known as cation complexation, as proposed by Courty et al. [17], was used for the preparation of the ceria-gadolinia solid solution. This method has the advantage of low cost and relative simplicity. Moreover, this technique generates less carbon residues than other similar techniques of synthesis, and it has proved to be quite effective to produce highly sinterable ceramic powders [18].

2. Experimental

Cerium nitrate hexahydrate (99.99%, Aldrich) and gadolinium oxide (99.9%, Aldrich) were used as starting materials. Other reagents were anhydrous citric acid (99.5%), and nitric acid (65%, P.A.). A stock solution (2 mol l^{-1}) of cerium nitrate was prepared by slow dissolution of the starting material in deionized water. The gadolinium nitrate solution was prepared by dissolving the corresponding oxide in a nitric acid solution. Another solution containing citric acid as a complexant agent was added to the mixed solution. The molar ratio metal:citric acid was set to 1:2. After homogenization of this solution, the temperature was raised to 80 °C, and maintained under stirring to remove excess water and to convert it to a transparent gel. While raising the temperature, the solution became more viscous with evolution of foam, and finally it gelled without any visible formation of precipitation or turbidity. Keeping the solution at this temperature, there is an increase of the viscosity with simultaneous elimination of water and NO_2.

The initial thermal decomposition of the precursor was carried out at 250 °C for 1 h. The resulting ash-like material was afterwards pyrolyzed at 400 or 600 °C for 1 h. Cylindrical pellets of 12 mm in diameter and 1–2 mm in thickness were prepared by uniaxial pressing at 98 MPa in a steel die. The sintering of pellets was performed at 1500 °C for 3 h in air. The nominal Gd_2O_3 content in the sintered material was 11.1 mol%.

The thermal decomposition of the organic precursor was studied by simultaneous thermogravimetry (TG), and differential thermal analysis (DTA) (STA 409, Netzsch) up to 1200 °C, heating at a rate of 10 °C min^{-1} in synthetic air (~20% O_2). Alumina (Alumalux, Alcoa) was used as reference material. Fourier transform infrared spectroscopy, FT-IR, was also used to follow the decomposition of the precursor material, using a He–Ne laser in the wavenumber interval from 400 to 4000 cm^{-1} (Magna IR560, Nicolet). Transparent pellets were prepared by pressing an intimate mixture obtained by shaking the powder specimen and KBr.

The residual carbon content was determined (CS400, Leco) in calcined powders after mixing them with a low melting point material. The distribution of particle sizes was measured by laser scattering (model 1064, Cilas) using sodium pyrophosphate as dispersing agent. The specific surface area was analyzed using five-point Brunauer, Emmett and Teller (BET), analysis by nitrogen adsorption (ASAP 2010, Micromeritics). X-ray diffraction (D8 Advance, Bruker-AXS) methods were used for phase

analysis and crystallite size determination. The crystallite size, d_{XRD}, of the calcined powders was estimated using the Scherrer equation:

$$d_{XRD} = \frac{0.9\lambda}{\beta \cos\theta} \quad (1)$$

where λ is the wavelength of the X-rays, and θ is the scattering angle of the main reflection (1 1 1) [19]. High-grade silicon powder was used as standard to account for instrument broadening correction. Scanning electron microscopy (SEM) (XL30, Philips) was used to observe the morphology of powder particles and of fractured surfaces in sintered pellets. Apparent sintered densities were obtained by the Archimedes principle using water as immersing medium.

3. Results and discussion

The as-prepared material proved to be hygroscopic in nature; thus, before measurements, it was maintained at 45 °C. The DTA/TG curves of the precursor metal complex are shown in Fig. 1. The DTA curve exhibits an endothermic peak around 100 °C, and a large exothermic peak starting at ~330 °C and extending up to ~400 °C. The temperature of the endothermic peak is near the boiling point of water, so it can be assigned to the desorption of physically adsorbed water from the precursor. The exothermic evolution can be ascribed to the burn out of organic material, and to the crystallization of the solid solution. In previous works [20,21] using this technique to prepare other ceramic materials, the exothermic events were related to the liberation of NO_x, CO, CO_2 and water vapor as major components.

There are two steps in the TG curve, and the total weight loss up to 430 °C is 61%. The first step in the weight loss occurs from ~90 to ~140 °C, and correlates with the endothermic peak in the DTA curve. It was proposed earlier [22,23] that the weight loss in this temperature range is due not only to the desorption of water, but also to the release of free citric acid. The presence of free citric acid and metal nitrates in the metal complex precursor could account for its hygroscopic nature. The final step of weight loss occurs continuously indicating a decomposition reaction of type I. It is known from the literature [22,24] that metal complexes prepared by this technique may present two main types of decomposition reactions. Type I is characteristic of a continuous weight loss, whereas type II is a

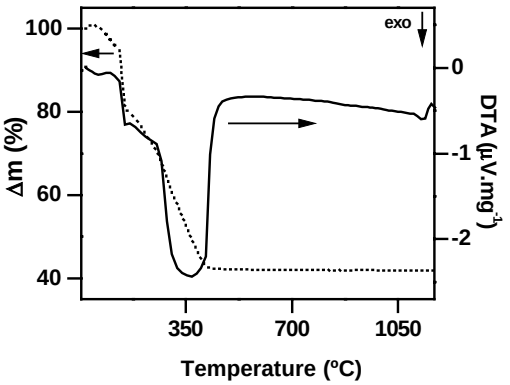

Fig. 1. DTA/TG curves of the metal complex precursor.

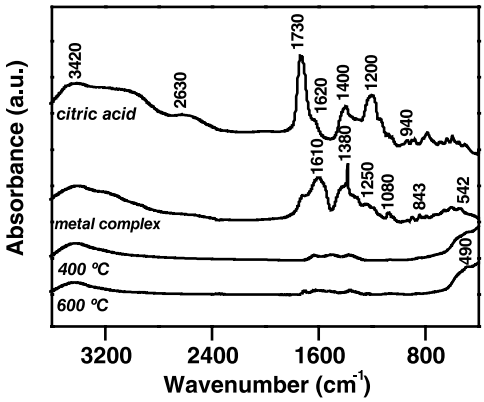

Fig. 2. FT-IR spectra of the precursor material, metal complex and pyrolyzed powders.

stepwise reaction due to the formation of an intermediate complex. The main difference between these decomposition reactions is the relative stability of the precursor.

In order to obtain a better insight in the structure and composition of the precursor and to characterize the metal complex-to-ceramic conversion, FT-IR spectroscopy was performed before and after the pyrolysis of the precursor material. Fig. 2 shows FT-IR of citric acid, metal complex precursor, and calcined powders at 400 and 600 °C. The infrared absorption spectrum of citric acid exhibits infrared absorption bands related to the presence of OH groups (~3420 cm^{-1}), OH stretching vibrations (~2630 cm^{-1}), C=O stretching (~1730 cm^{-1}), COO^- vibration (~1620 cm^{-1}), COO^- stretching (1400 cm^{-1}), C–O stretching or OH deformation (1200 cm^{-1}), and out-of-plane OH bend (940 cm^{-1}). In the metal complex precursor spectrum the main observed bands are related to COO^- vibration of a metal chelate (~1610 cm^{-1}), and nitrate ions (1380 and 843 cm^{-1}). The band at ~500 cm^{-1} is characteristic of metal–oxygen vibrations. The presence of free citric acid in the precursor material cannot be ascertained once the corresponding infrared band (3500 cm^{-1}) overlaps that of OH groups. After calcination at 400 or 600 °C, most of the infrared absorption bands disappeared. However, low-intensity bands due to carbon–oxygen bonds and that of metal–oxygen bond were detected.

Table 1 shows determined values of carbon content in calcined powders. The residual carbon content decreases with increasing the calcination temperature. However, these figures are relatively low when compared to results obtained for other materials prepared by the same technique [22,24,25]. This result is attributed to the low heating rate (2 °C min^{-1}) used during thermal treatments.

Fig. 3 shows the particle size distribution curves obtained by laser scattering for calcined powders. The shape of the distribution is similar, but the size interval is different for both powders. The equivalent spherical diameter, d_{50}, obtained at 50% mass finer is shown in Table 1. From these results,

Table 1
Values of residual carbon content (C, %), equivalent spherical diameter (d_{50}), specific surface area (S), and crystallite size (d_{XRD}) after the pyrolysis of the precursor at 400 and 600 °C

Pyrolyzed at (°C)	C (%)	d_{50} (μm)	S (m^2 g^{-1})	d_{XRD} (nm)
400	0.42	5.4	31.8	6.5
600	0.30	1.3	44.4	9.5

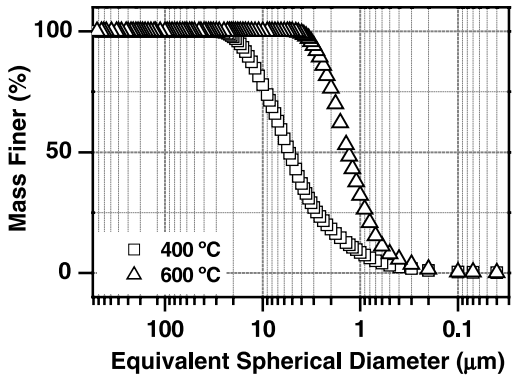

Fig. 3. Particle size distribution of pyrolyzed powders.

it can be inferred that the average particle size of the solid solution decreases with increasing the temperature of pyrolysis. In general, the increase in the calcination temperature produces an increase in the degree of agglomeration of the powder particles, and an opposite trend to that of Fig. 3 is obtained. As will be shown below, this unusual result is a consequence of the particle morphology formed during the pyrolysis of the metal complex precursor.

The specific surface area values after calcination at 400 and 600 °C are shown in Table 1. The relatively high values obtained indicate that this technique of synthesis produces reactive powders. It is worth to note that increasing the calcination temperature there is an increase in the specific surface area of the particulate material. This means that there is a decrease in the particle size with increasing the pyrolysis temperature, and correlates with results of particle size distribution.

X-ray diffraction patterns obtained for the metal complex precursor, partially decomposed material and after calcination at 400 and 600 °C are shown in Fig. 4. The metal complex precursor is amorphous to X-rays, whereas after its partial decomposition at 250 °C it is crystalline. However, the diffraction peaks are relatively broad indicating that the powder is composed of very small crystallites. The broadening of the peaks gradually decreases with increasing the temperature of pyrolysis.

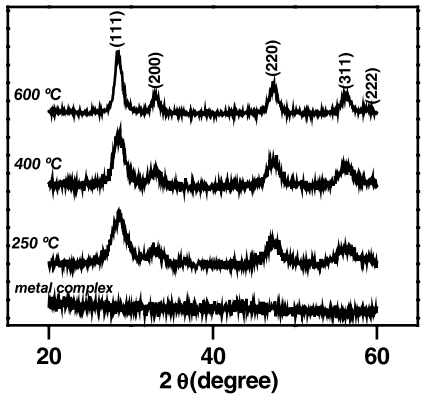

Fig. 4. X-ray diffraction patterns of the metal complex precursor, partially decomposed material and pyrolyzed powders.

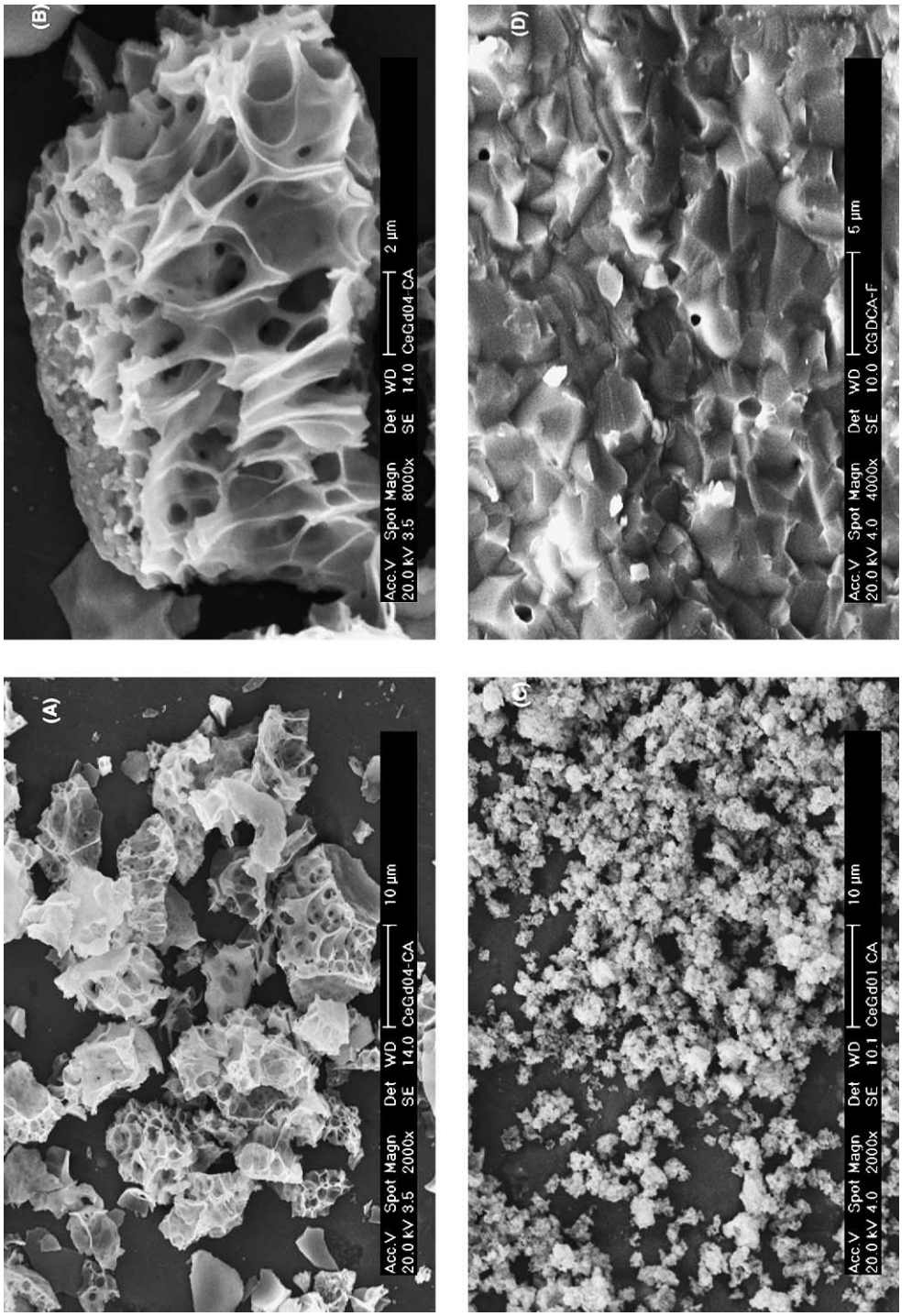

Fig. 5. SEM micrographs of pyrolyzed powders (A, B, C) and fractured surface (D).

The crystallite size determined from the Scherrer equation for the calcined powders is shown in Table 1. These low values for both temperature of pyrolysis of the metal complex show that particles of the solid solution in the nanosize range were obtained for both temperatures.

SEM micrographs of pyrolyzed powders are shown in Fig. 5. The morphology of powder calcined at 400 °C shows a very porous structure, as can be seen in Fig. 5A. In addition, large particles were formed as shown with high magnification in Fig. 5B. These large particles are porous and were probably formed by the liberation of CO_2 and water from the decomposition of citric acid. Increasing the temperature of pyrolysis to 600 °C, the morphology of powder particles changed (Fig. 5C). The magnification in Fig. 5A and C are the same, so it can be seen that the particle size decreases with increasing the calcination temperature. This feature may be explained as a result of the liberation of residual carbon entrapped into the porous structure. The pressure exercised by gaseous species should be responsible for the break up of the porous structure of large particles. These morphological changes with the calcination temperature explain the behavior of the particle size distribution and specific surface area.

It should be emphasized that the crystallite (or primary particle) size seems not to be influenced by the particle morphology.

Powder compacts were prepared from powders calcined at 600 °C, and sintered at 1500 °C for 3 h. Fig. 5D shows a SEM micrograph of a fractured surface of a sintered powder compact. The main microstructure features are a transgranular fracture mode along with closed porosity. These microstructure observations are typical of a high strength compact in the final stage of the sintering process.

The relative density of sintered compacts reached 99.2%. The high densification attained is significant when compared to general literature data [9,13–15] on powders prepared by similar wet-chemical methods.

4. Conclusions

Nanosized powders of gadolinia-doped ceria were prepared by the pyrolysis of a metal complex precursor using citric acid as complexant agent. The temperature of the gel decomposition should be suitably chosen to break up the porous structure formed, enabling the evolution of entrapped gaseous species. Sintered specimens with high densification may be obtained using this low-cost and relatively simple technique of synthesis.

Acknowledgements

To FAPESP (95/05172-4, 96/09604-9, 97/06152-2), CNPq (300934/94-7), FINEP/PRONEX, and CNEN for financial support. To the Metallic and Ceramic Processing Center and Gas Analysis Laboratory at IPEN. R.A. Rocha acknowledges FAPESP (99/12494-9) for the scholarship.

References

[1] B.C.H. Steele, Solid State Ionics 129 (2000) 95.
[2] A.E.C. Palmqvist, M. Wirde, U. Gelius, M. Muhammed, Nanostructured Mater. 11 (1999) 995.

[3] T.H. Etsell, S.N. Flengas, Chem. Rev. 70 (1970) 339.
[4] H. Inaba, H. Tagawa, Solid State Ionics 83 (1996) 1.
[5] B.C.H. Steele, J.A.K. Zheng, J. Bae, in: Proceedings of the Second International Conference on Ceramics in Energy Applications, Institute of Energy, London, 1994, p. 109.
[6] S. Wang, H. Inaba, H. Tagawa, T. Hashimoto, J. Electrochem. Soc. 144 (1997) 4077.
[7] N. Maffei, A.K. Kuriakose, Solid State Ionics 107 (1998) 67.
[8] I. Riess, D. Braunshtein, D.S. Tannhause, J. Am. Ceram. Soc. 64 (1981) 479.
[9] A.L. Dragoo, C.K. Chiang, in: F. Salzano (Ed.), Proceedings of the Conference on High Temperature Solid Oxide Electrolytes, Brookhaven National Laboratory, Upton, USA, 1983, pp. 268–281.
[10] J. Van Herle, T. Horita, T. Kawada, N. Sakai, H. Yokokawa, M. Dokiya, Solid State Ionics 86–88 (1996) 1255.
[11] S.J. Hong, K. Mehta, A.V. Virkar, J. Electrochem. Soc. 145 (1998) 638.
[12] K. Yamashita, K.V. Ramanujachary, M. Greenblatt, Solid State Ionics 81 (1995) 53–60.
[13] M. Mogensen, T. Lindegaard, V.R. Hansen, G. Mogensen, J. Electrochem. Soc. 141 (1994) 2122.
[14] N. Kim, B.-H. Kim, D. Lee, J. Power Sources 90 (2000) 139.
[15] K. Huang, M. Feng, J.B. Goodenough, J. Am. Ceram. Soc. 81 (1998) 357.
[16] M. Pechini, US Patent 3,330,697 (1967).
[17] P. Courty, B. Delmon, C. Marcilly, A. Sugier, Fr. Patent 1604707 (1968).
[18] E.N.S. Muccillo, R.A. Rocha, R. Muccillo, Mater. Lett. 53 (2002) 353.
[19] B.E. Warren, X-Ray Diffraction, Dover, New York, 1990, p. 258.
[20] C. Marcilly, P. Courty, B. Delmon, J. Am. Ceram. Soc. 53 (1970) 56.
[21] H. Taguchi, S.-I. Matsu-ura, M. Nagao, T. Choso, K. Tabata, J. Solid State Chem. 129 (1997) 60.
[22] P. Courty, H. Ajot, C. Marcilly, Powder Technol. 7 (1973) 21.
[23] M.S.G. Baythoun, F.R. Sale, J. Mater. Sci. 17 (1982) 2757.
[24] C.-T. Chu, B. Dunn, J. Am. Ceram. Soc. 70 (1987) C375.
[25] S.W. Kwon, S.B. Park, G. Seo, S.T. Hwang, J. Nucl. Mater. 257 (1998) 172.